ERID 098076

Pergamon

Geochimica et Cosmochimica Acta, Vol. 63, No. 11/12, pp. 1653–1660, 1999

0016-7037/99 $20.00 + .00

PII S0016-7037(99)00089-7

High precision iron isotope measurements of terrestrial and lunar materials

BRIAN L. BEARD* and CLARK M. JOHNSON
Department of Geology and Geophysics, University of Wisconsin-Madison, Madison, Wisconsin 53706, USA

(*Received August 5, 1998; accepted in revised form February 11, 1999*)

Abstract—We present the analytical methods that have been developed for the first high-precision Fe isotope analyses that clearly identify naturally-occurring, mass-dependent isotope fractionation. A double-spike approach is used, which allows rigorous correction of instrumental mass fractionation. Based on 21 analyses of an ultra pure Fe standard, the external precision (1-SD) for measuring the isotopic composition of Fe is ±0.14 ‰/mass; for demonstrated reproducibility on samples, this precision exceeds by at least an order of magnitude that of previous attempts to empirically control instrumentally-produced mass fractionation (Dixon et al., 1993). Using the double-spike method, 15 terrestrial igneous rocks that range in composition from peridotite to rhyolite, 5 high-Ti lunar basalts, 5 Fe-Mn nodules, and a banded iron formation have been analyzed for their iron isotopic composition. The terrestrial and lunar igneous rocks have the same isotopic compositions as the ultra pure Fe standard, providing a reference Fe isotope composition for the Earth and Moon. In contrast, Fe-Mn nodules and a sample of a banded iron formation have iron isotope compositions that vary over a relatively wide range, from $\delta^{56}Fe = +0.9$ to -1.2 ‰; this range is 15 times the analytical errors of our technique. These natural isotopic fractionations are interpreted to reflect biological ("vital") effects, and illustrate the great potential Fe isotope studies have for studying modern and ancient biological processes. *Copyright © 1999 Elsevier Science Ltd*

1. INTRODUCTION

Mass-dependent fractionation of light stable isotopes, such as C, O, N, and S, are a well studied phenomenon (e.g., Hoefs, 1987). Isotopic fractionation of the light stable isotopes are controlled by temperature, phase transitions (e.g., liquid to vapor), inter-mineral equilibrium fractionation, and biological activity (e.g., Friedman and O'Neil, 1977; Schidlowski et al., 1983). Determining the relative contributions of isotopic fractionation for the light stable isotopes in terms of inorganic (e.g., temperature or phase effects) and organic factors (e.g., "vital" effects) is difficult because both can be significant due to the large relative mass differences between the isotopes.

In contrast, the isotopic composition of the first transition metals may be useful in evaluating kinetically-controlled, biologically-induced isotope fractionation, because it is anticipated that their small relative mass differences, as compared to the well-studied light stable isotopes, will produce minimal or unmeasureable inorganic (equilibrium) isotope fractionation. Iron is a critically important element in biological processes, and has a relative mass difference that is likely to be sufficient to record biologically-produced isotopic fractionation, and yet is expected to be minimally fractionated by inorganic (equilibrium) processes. Iron availability is one of the most important controlling factors for organic productivity in the oceans (e.g., Martin and Fitzwater, 1988). Moreover, iron biominerals are ubiquitous in nature (Lowenstam, 1981), and are produced by iron-reducing, iron oxidizing, and magnetotactic bacteria as well as higher life forms such as Chiton. Indeed, iron biominerals have been inferred to exist in ancient rocks from Mars (McKay et al., 1996).

Precise isotopic analysis of the transition metals is analytically challenging, because the most widely available appropriate instrumentation is thermal ionization mass spectrometry (TIMS), which produces significant mass fractionation during isotopic analysis. In this contribution, we use a double-spike approach to remove instrumentally-produced mass fractionation; these methods have produced the most precise measurements of the isotopic composition of Fe that preserve mass-dependent fractionation, and demonstrates that Fe isotopes vary in nature as a result of mass-dependent fractionation.

2. PREVIOUS IRON ISOTOPE STUDIES

Estimates for the atomic abundances of the stable isotopes of Fe (^{54}Fe 5.84%, ^{56}Fe 91.76%, ^{57}Fe 2.12%, ^{58}Fe 0.28%) have been made by a number of workers (Valley and Anderson, 1947; Völkening and Papanastassiou, 1989; Taylor et al., 1992; Dixon et al., 1993). The two biggest challenges in making precise Fe isotope ratio measurements that retain naturally-produced isotope variations are the low ionization efficiency of iron and the necessity to correct for instrumental mass fractionation.

Corrections for instrumentally-produced mass fractionation that preserve natural, mass dependent fractionation can be approached in one of two ways- a double-spike method, which allows for rigorous calculation of instrumental mass fractionation (e.g., Compston and Oversby, 1969; Eugster et al., 1969; and Gale, 1970), or an empirical adjustment, based on comparison with isotopic analysis of standards. The empirical approach assumes that standards and samples fractionate to the same degree during isotopic analysis, requiring carefully controlled analysis conditions. Such approaches are commonly used for Pb isotope work. Certified standard material of known Fe isotope composition (determined using gravimetrically prepared standards) has recently become available (Taylor et al.,

*Author to whom correspondence should be addressed (beardb@geology.wisc.edu).

Table 1. Collector configuration used for static multicollector analysis of Fe isotope ratios.*

	Low 2	Low 1	Axial	High 1	High 2	High 3	High 4
Background	51.5	52.5	53.5	54.5	55.5		56.5
Scan 1	^{52}Cr		^{54}Fe		^{56}Fe		
Scan 2		^{56}Fe	^{57}Fe	^{58}Fe			^{60}Ni

* The Micromass Sector 54 collector block is designed for a working range in mass spread of 9.5%. To simultaneously analyze all four Fe isotopes and continuously monitor for Cr and Ni isobars would require a relative mass spread of 14.4%. Therefore, 2 multi-collection scans are used. A beam growth correction using the ion intensity measured for ^{56}Fe in scans 1 and 2 is used for measurement of the ^{54}Fe/^{57}Fe and ^{54}Fe/^{58}Fe ratios.

1993). Using these certified reference materials, Dixon et al. (1993) report Fe isotope ratio precisions of ±0.3‰/mass for standard Fe material. However, it is important to stress that the precision and accuracy of Fe isotope ratios determined on unknown samples may be very difficult to evaluate because each filament load in a TIMS analysis is different, and, in the case of Fe, important and variable matrix and interference effects are present. The Fe isotope data reported by Dixon et al. (1992) are significantly more variable than those of standards, and contain internal inconsistencies among the isotope ratios, suggesting that their practical precision is more on the order of ±1 to 3‰/mass difference, using their empirical approach.

We consider rigorous correction for instrumental mass bias to be a prerequisite for evaluating if naturally occurring mass-dependent isotope fractionation occurs. This concept is well illustrated by the definitive Ca isotope work of Russell et al. (1978), which used a double-spike approach. Prior to the Ca isotope investigation of Russell et al. (1978), natural, mass-dependent Ca isotope variations were estimated to be large (12‰/mass based on an empirical method for instrumental mass-fractionation correction; e.g., Miller et al., 1966). However, Russell et al. (1978) showed that naturally-occurring, mass-dependent variations in Ca isotopes is much smaller (total range of 0.6‰/mass), and that the previously reported mass-dependent variations were entirely a result of imprecise corrections for instrumental mass fractionation. We suspect that variations in instrumental mass fractionation correction from sample to sample is likely to be more problematic for Fe isotope measurements, as compared to Ca, because of the low ionization efficiency of Fe.

3. CHEMICAL PROCESSING OF FE FOR ISOTOPIC ANALYSIS

Samples were dissolved using standard techniques; bulk rock silicates were dissolved using a 5:1 mixture of concentrated HF and HNO_3 in sealed Savillex Teflon beakers, and Fe-Mn nodules were dissolved using 6M HCl. A complete dissolution of Fe-Mn nodules was not used to avoid dissolving silicate inclusions. The high-Ti lunar basalts are bulk cation cuts that were saved from previous Hf isotope studies (Beard et al., 1998a). Following dissolution, silicate samples were converted to chloride salts by evaporating the acids used for dissolution, adding 6M HCl, and heating overnight in sealed Teflon beakers.

Iron was separated from the rest of the rock matrix using anion exchange resin and HCl (e.g., Strelow, 1980). Column-yield tests using between 100 and 10,000 μg of Fe indicate a recovery of 80%. The bulk of the Fe loss occurs over a long tail as Fe is eluted from the anion exchange resin using 1M HCl. Iron isotope fractionation during anion-exchange chromatographic separation is not believed to be significant. The isotope composition of the J-M Fe processed using anion exchange chromatography is the same as that measured for J-M Fe taken directly from the stock solution. Moreover, the isotope composition of J-M Fe eluted from a small part of the tail of the Fe peak during elution of Fe by 1M HCl (last 5% of the total Fe removed from the anion exchange column) is the same as that for J-M Fe from the stock solution. Separation of Fe is essentially a one stage process because of the very high affinity of ferric iron for resin at high molarity HCl. Moreover, short columns are used (resin height is approximately 2 cm), making it unlikely that significant isotope fractionation could occur.

Total blanks for our procedure average 40 ng of Fe, producing a sample to blank ratio of ~2,500 to ~75,000, making the blank contribution entirely negligible. The bulk of the total procedural blanks are from the HF and HNO_3 that are used in the dissolution of silicates. Procedural blanks for the ion-exchange chemistry average 5 nanograms. All reagents used were prepared in a class-100 clean lab. Hydrofluoric, HNO_3, and HCl were prepared by sub-boiling distillation of analytical reagent-grade acid. Water was purified by reverse osmosis and then ion-exchange chromatography using a Nanopure water-purification system. The silica gel and H_3PO_4 used for loading filaments are ultra pure reagents (Seastar chemicals). Iron blanks for water and HCl average 0.1 and 0.3 ng, respectively. Iron blanks for HF and HNO_3 are 9 and 1.6 ng, respectively. Loading blanks average 0.3 ng.

4. MASS ANALYSIS OF FE

All isotope analyses were conducted at the University of Wisconsin Radiogenic Isotope Laboratory using a Mircomass Sector 54 mass spectrometer. This instrument is fitted with 7 Faraday collectors and an analog Daly detector.

4.1. Sample Loading

The filament ribbon used for Fe isotope analysis is 99.999% pure ("zone-refined") Re. After adding an Al_2O_3 slurry to a single blank filament, the Fe sample (~4 μg of Fe) is loaded, followed by 1M H_3PO_4, followed by silica gel. This loading recipe was chosen after evaluating the Boric acid-silica gel technique used by Götz and Heumann (1988), Völkening and Papanastassiou (1989), and Dixon et al. (1993). The Al_2O_3 slurry emitter produces longer lasting and more stable ion

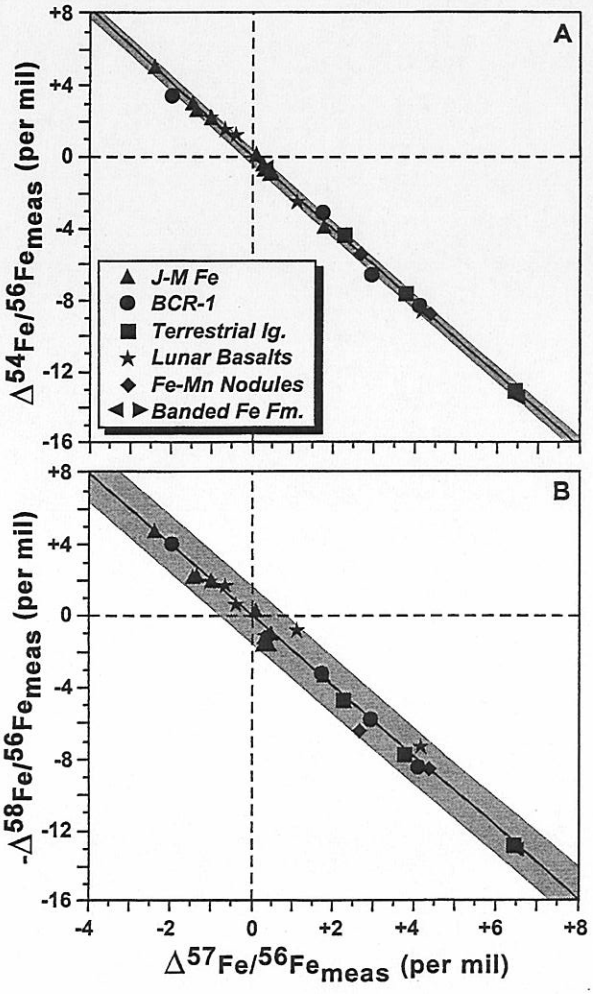

Fig. 1. Range in average measured (fractionated) isotope ratios of unspiked samples, plotted as the per mil deviation (Δ) from the true ratios. These trends illustrate the magnitude of instrumentally-produced mass fractionation using TIMS, on the order of 8 per mil/mass. All data plot along the same mass-dependent fractionation curve. Bands indicate 2-standard deviations error envelopes (note larger errors in $^{58}Fe/^{56}Fe$). A) plot of $^{54}Fe/^{56}Fe$ versus $^{57}Fe/^{56}Fe$ and B) $^{58}Fe/^{56}Fe$ vs $^{57}Fe/^{56}Fe$ of unspiked samples.

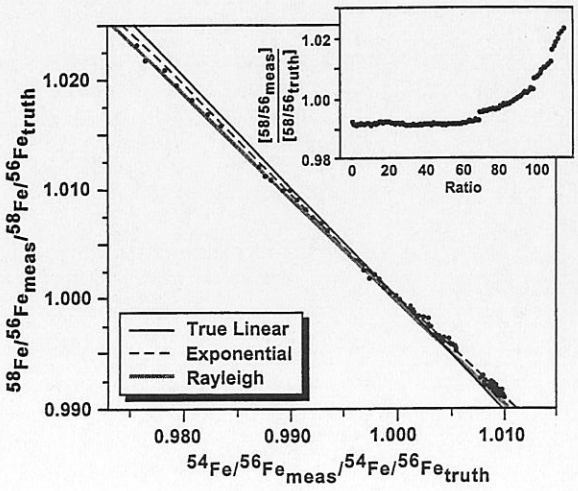

Fig. 2. Plot of the $[^{54}Fe/^{56}Fe]_{measured}/[^{54}Fe/^{56}Fe]_{truth}$ versus $[^{56}Fe/^{58}Fe]_{measured}/[^{56}Fe/^{58}Fe]_{truth}$ of a representative run of the equal atom Fe standard. Lines show the true linear law, exponential law, and Rayleigh distillation law mass-fractionation curves. Instrumental mass-fractionation is best approximated using an exponential law for the first 2/3 to 3/4 of the data taken in a typical analysis. Inset shows the $[^{56}Fe/^{58}Fe]_{measured}/[^{56}Fe/^{58}Fe]_{truth}$ from the beginning to the end of the run; only when the mass fractionation becomes extreme does it appear to follow a Rayleigh distillation law.

beams and high ion currents ($>2 \times 10^{-11}$ A total current) as compared to the Boric acid-silica gel technique (T. Bullen, pers. commun., 1997). A triple filament loading procedure was also tried, but large ion currents were not as stable and required an order of magnitude larger amount of Fe to produce large ion signals that were similar to the ion intensities obtained using the single filament assembly.

4.2. Mass Analysis Conditions

Mass analysis utilizes a 2-scan, multi-collector routine, in addition to a background scan (Table 1). Ten to 12 blocks (10 sets of scans each) of data are collected; the ion beam is focused, peak centered, and the filament current is adjusted between each block. Two on-peak integrations are required to analyze all 4 isotopes of iron and simultaneously monitor Cr and Ni isobars (Table 1) because the total relative mass spread (14.4%) is larger than that available in the current generation of multi-collector TIMS instruments. A simple linear correction for beam growth between the scans is applied using ^{56}Fe. The relative mass difference of Fe is large enough that there is not enough overlap to collect both ^{57}Fe in the H4 Faraday collector of scan 1 and ^{60}Ni of scan 2. Moreover, it is not possible to get the H3 and H4 Faraday collectors close enough to one another to analyze both ^{57}Fe using H4 in scan 1 and ^{60}Ni using H3 in scan 2.

The 2-scan collector configuration is the best compromise between the mass dispersion limits of the multi-collector array and keeping the key Faraday collectors (L1, axial, H1, and H2) relatively close to the axial collector; this later factor is increasingly recognized as being important in high-precision isotopic analyses of low- to moderate-mass (high dispersion) elements. Keeping the Faraday collectors that are used for the Fe masses close to the axial position is important for minimizing optical aberrations that may be present due to irregularities in the focal plane or imperfections in focus conditions or peak shapes. Similar conclusions regarding coincidence of the ion focal plane with that of Faraday collectors at large mass dispersion have been made for Ca isotope analyses; Skulan et al. (1997) indicate that the external precision of Ca isotope analysis is better using a single-collector, peak-hopping routine as opposed to a static multi-collection routine because ion optic problems are minimized.

Isobaric interferences caused by ^{54}Cr and ^{58}Ni are monitored using ^{52}Cr and ^{60}Ni, respectively. Corrections for these isobars are made using $^{54}Cr/^{52}Cr = 0.0282$ and $^{58}Ni/^{60}Ni = 2.616$. The ^{54}Cr correction on ^{54}Fe is typically 0.002% at the beginning of

Table 2. Corrected iron isotope compositions of terrestrial and lunar igneous rocks.*

Sample description	Material analyzed	$^{54}Fe/^{56}Fe$	% error	$^{57}Fe/^{56}Fe$	% error	$^{58}Fe/^{56}Fe$	% error	$\delta^{56}Fe$	Error (‰)
Grizzly Peak Tuff, Colorado									
FG-1 Rhyolite	Biotite	0.063676	0.0352	0.023089	0.0171	0.0030617	0.0339	0.11	0.35
		0.063679	0.0202	0.023088	0.0098	0.0030616	0.0194	0.06	0.20
FG-3 Dacite	Biotite	0.063701	0.0239	0.023084	0.0116	0.0030606	0.0231	−0.28	0.24
		0.063680	0.0223	0.023088	0.0109	0.0030615	0.0205	0.05	0.22
FG-5 Andesite	Biotite	0.063699	0.0224	0.023085	0.0108	0.0030607	0.0217	−0.25	0.22
		0.063675	0.0220	0.023089	0.0107	0.0030617	0.0212	0.12	0.22
FG-7 Bas. Andesite	Hornblende	0.063719	0.0167	0.023081	0.0082	0.0030597	0.0161	−0.57	0.17
Rio Hondo Pluton, Latir volcanic field, New Mexico									
Q82J-33 Granite	Biotite	0.063670	0.0124	0.023090	0.0060	0.0030620	0.0120	0.20	0.12
		0.063696	0.0172	0.023085	0.0084	0.0030608	0.0166	−0.21	0.17
Q827-8 Granite	Biotite	0.063692	0.0128	0.023086	0.0062	0.0030610	0.0123	−0.14	0.13
Big Pine volcanic field, California									
BP9220B Rhyolite	Bulk rock	0.063691	0.0132	0.023086	0.0064	0.0030610	0.0128	−0.13	0.13
Pi-2-101 Basalt	Bulk rock	0.063678	0.0235	0.023089	0.0115	0.0030618	0.0227	0.12	0.24
		0.063680	0.0221	0.023088	0.0108	0.0030615	0.0214	0.04	0.22
Pi-2-6 Peridotite xeno	Olivine	0.063665	0.0104	0.023091	0.0051	0.0030622	0.0100	0.28	0.10
Columbia River Flood basalts/Snake River Plane basalts Northwestern U.S.A.									
UMAT-1	Bulk rock	0.063713	0.0140	0.023082	0.0068	0.0030600	0.0136	−0.46	0.14
H-9-36a	Bulk rock†	0.063691	0.0157	0.023086	0.0077	0.0030610	0.0152	−0.13	0.16
H-8-91	Bulk rock†	0.063685	0.0100	0.023087	0.0049	0.0030613	0.0097	−0.04	0.10
HSR-16	Bulk rock†	0.063699	0.0124	0.023085	0.0061	0.0030607	0.0120	−0.25	0.12
BCR-1	Bulk rock	0.063696	0.0282	0.023085	0.0137	0.0030608	0.0272	−0.21	0.28
		0.063677	0.0114	0.023088	0.0055	0.0030617	0.0110	0.10	0.11
		0.063701	0.0255	0.023084	0.0124	0.0030605	0.0246	−0.29	0.25
		0.063665	0.0188	0.023091	0.0092	0.0030622	0.0182	0.28	0.19
		0.063699	0.0172	0.023085	0.0084	0.0030607	0.0166	−0.25	0.17
		0.063696	0.0268	0.023085	0.0130	0.0030608	0.0258	−0.20	0.27
		0.063710	0.0209	0.023083	0.0102	0.0030602	0.0202	−0.42	0.21
Proterozoic meta-komatiitic basalt, Colorado									
PS-7.9-87	Bulk rock	0.063678	0.0161	0.023088	0.0078	0.0030616	0.0155	0.08	0.16
		0.063702	0.0117	0.023084	0.0057	0.0030605	0.0113	−0.31	0.12
High-Ti lunar basalts									
7858,61	Bulk rock†	0.063685	0.0376	0.023087	0.0183	0.0030613	0.0363	−0.03	0.38
		0.063665	0.0123	0.023090	0.0060	0.0030622	0.0119	0.28	0.12
71545,16	Bulk rock†	0.063691	0.0227	0.023086	0.0111	0.0030610	0.0220	−0.13	0.23
		0.063638	0.0154	0.023095	0.0075	0.0030635	0.0149	0.70	0.15
		0.063676	0.0170	0.023089	0.0083	0.0030617	0.0164	0.12	0.17
77516,22	Bulk rock†	0.063685	0.0233	0.023087	0.0114	0.0030613	0.0225	−0.03	0.23
		0.063697	0.0166	0.023085	0.0081	0.0030607	0.0160	−0.23	0.17
10044,634	Bulk rock†	0.063671	0.0203	0.023089	0.0099	0.0030620	0.0196	0.19	0.20
10047,219	Bulk rock†	0.063666	0.0207	0.023090	0.0101	0.0030622	0.0200	0.26	0.21
		0.063666	0.0154	0.023090	0.0075	0.0030622	0.0148	0.26	0.15

* The quoted errors are internal-run statistics calculated from individual block analyses of the mixture aliquot. Replicate analyses are from different mass spectrometry runs of separate filament loads. Replicate analyses for BCR-1 include 4 different spike to sample mixture aliquots. The symbol (†) indicates analysis of residue after Hf extraction; see Beard et al. (1998a) for details of chemical processing of samples for Hf chemistry.

the analysis and drops to 0 by the end of the analysis. Nickel isobaric interferences, when present (10% of the analyses), burned off during the course of the run and at most required a 0.01% correction. Both Cr and Ni have much higher ionization efficiencies than Fe, and these isobars are always burned off during the course of a TIMS run, typically before an Fe isotope analysis is started.

4.3. Calculation of Fractionation-Corrected Isotopic Compositions

In its most general application, where the isotopic composition of the sample is completely unknown, the double-spike procedure requires analysis of an unspiked aliquot and a spiked aliquot. However, if isotopic variations are only a result of naturally-occurring, mass-dependent fractionation, the unspiked aliquot does not need to be measured for each sample, once the natural isotopic variation of a particular reservoir is characterized (e.g., Russell et al., 1978). This simplification is robust and will not produce any bias in the results unless a) the natural-occurring mass fractionation is very large and follows a different mass-dependent fractionation law from that used to correct instrumental mass fractionation (e.g., linear law versus Rayleigh distillation), and b) the unknown sample does not lie on the natural fractionation curve of the assumed reservoir. The first factor is entirely negligible for natural isotope variations on the order of several per mil. The second factor may be significant for different planetary bodies or nucleosynthetic reservoirs; this is perhaps best illustrated for oxygen isotopes, where terrestrial and lunar samples lie on a $^{18}O/^{16}O$–$^{17}O/^{16}O$

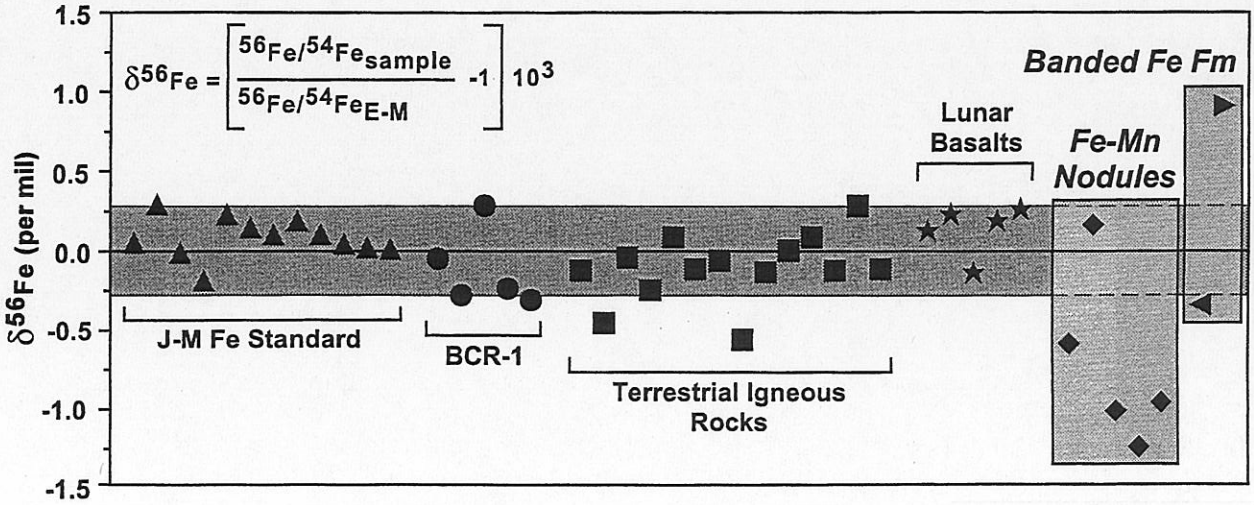

Fig. 3. δ^{56}Fe values measured for the J-M Fe standard, terrestrial igneous rocks, lunar high-Ti basalts, Fe-Mn nodules, and a banded iron formation. Terrestrial and lunar igneous rocks have a constant Fe isotope composition that is the same as that measured for the J-M Fe standard. In contrast, Fe deposited in sedimentary environments have variable iron isotope compositions, which are thought to reflect biologically-produced mass fractionation. Horizontal band indicates the 1-standard deviation of the J-M Fe, BCR-1, terrestrial igneous and lunar samples. Duplicate analyses are plotted as averages.

natural fractionation array that is distinct from that of some meteorite components or the planet Mars (Clayton, 1993).

The double-spike corrected Fe isotope compositions of samples was calculated using a fixed isotopic composition for the unspiked aliquot, the average composition measured for J-M Fe. In fact, because all of the unspiked analyses plot along the same mass-dependent fractionation line (Fig. 1), any isotopic composition for the unspiked analysis, may be used for the double-spike solution, assuming it lies on the same natural fractionation trend. Such correlated variations in measured ratios are critical for evaluating data quality, and have not been demonstrated by previous Fe isotope studies that used emperical mass fractionation corrections (e.g., Dixon et al., 1992; 1993).

Absolute uncertainties in the spike isotope composition do not affect the precision of the double-spike solutions, but do affect the absolute values of the corrected Fe isotope composition of the samples. The confidence of relative differences in isotopic compositions for samples is therefore unaffected by the absolute uncertainty of the spike. The accuracy of absolute Fe isotope ratios for a sample, however, is linearly related to the accuracy of the spike isotopic composition; a 1‰/mass difference shift in the spike isotopic composition produces a one per mil/mass difference shift in the sample isotopic composition (although the relative isotopic difference between samples is unaffected).

All corrected Fe isotope ratios were calculated using a modified exponential mass fractionation law (the exponential law expanded into a power series and truncated after the first term for computational ease; Russel et al., 1978). The mass fractionation law that best describes intrumental fractionation associated with TIMS analysis of Fe isotopes was evaluated by analyzing an equal-atom standard made from enriched isotopic tracers of ^{54}Fe, ^{57}Fe, and ^{58}Fe (the J-M Fe standard was used as a ^{56}Fe "spike"). This approach is similar to that used by Hart and Zindler (1989) in their study of Ca isotope fractionation, and has the advantage that all isotope ratios are near unity, which eliminates errors in mass spectrometry that are due to large dynamic ranges or very low ion currents for low-abundance isotopes. Figure 2 shows the individual measured ^{54}Fe/^{56}Fe and ^{58}Fe/^{56}Fe ratios relative to the true isotopic composition of the equal-atom standard (as determined using the mixed U.W. ^{54}Fe–^{58}Fe spike). Individual ratios for a representative mass spectrometer run are shown, run at similar conditions as samples. The curves show the predicted trends for mass fractionation that follow a true linear law (e.g., Hart and Zindler, 1989), the exponential law (e.g., Russel et al., 1978), and a Rayleigh distillation law (e.g., Hart and Zindler, 1989). The data do not plot along a true linear law, but are better described by exponential or Rayleigh fractionation.

During the first 2/3 to 3/4 of an analysis, the data follow an exponential mass fractionation law, whereas in the latest parts of an analysis, usually when the ion beam is nearly exhausted, the data are better described by a Rayleigh distillation law. We therefore assume that, in general, instrumentally-produced mass fractionation of Fe isotopes using TIMS follows an exponential mass-fractionation law, as has been observed for Ca isotope analysis (e.g., Russell et al., 1978; Hart and Zindler, 1989).

Using an exponential approximation for the mass-fractionation law introduces an error of less than 0.1‰ in, for example, the ^{54}Fe/^{56}Fe ratio, over the range of instrumental fractionation that we measure and assuming that the true instrumentally-produced mass fractionation follows an exponential law. However, if a linear mass fractionation law is used, the errors introduced are on the order of 1‰ in the ^{54}Fe/^{56}Fe ratio, over the range of instrumental fractionation that we measure and

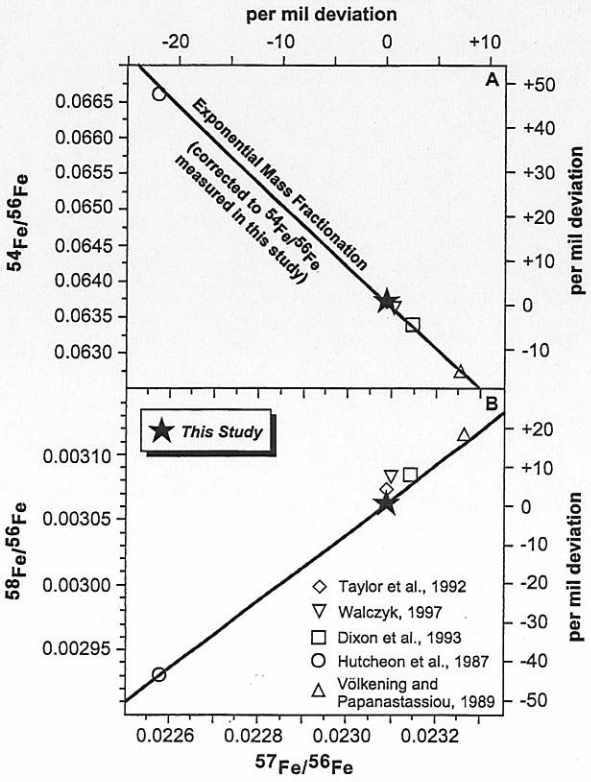

Fig. 4. Variations in absolute Fe isotope ratios for normal ("inorganic") Fe, as reported by Hutcheon et al., 1987; Völkening and Papanastassiou, 1989; Dixon et al., 1992, 1993; Taylor et al., 1992; Walczyk, 1997. The curve defines an exponential mass fractionation law, as calculated using our measured Fe isotope ratios for truth. Although the range in reported Fe isotope ratios for normal Fe is large, it is entirely a function of the choice of instrumental mass-fractionation correction. All of the reported normal Fe isotope compositions are identical to our measured ratios if corrected to our preferred isotope ratios, although the $^{58}Fe/^{56}Fe$ ratios of the other studies have significantly higher errors. A) Measured $^{54}Fe/^{56}Fe$ ratio versus measured $^{57}Fe/^{56}Fe$ ratios and, B) measured $^{58}Fe/^{56}Fe$ versus measured $^{57}Fe/^{56}Fe$ ratios.

assuming that the true instrumentally-produced mass fractionation follows an exponential law.

5. RESULTS OF FE ISOTOPE MEASUREMENTS

The J-M Fe standard has been measured to a precision of ±0.14‰/mass (1 SD), using 21 analyses of 12 mixtures, producing an average of $^{54}Fe/^{56}Fe$ of 0.063679 ± 0.0295%, $^{57}Fe/^{56}Fe$ of 0.023088 ± 0.0143% and a $^{58}Fe/^{56}Fe$ of 0.0030616 ± 0.0284%. Fifteen igneous rocks have been analyzed for their Fe isotope compositions; 8 of these samples have been analyzed in duplicate (Table 2). These igneous rocks range in composition from rhyolite to peridotite, and have the same iron isotope composition as that of the J-M Fe standard (Figure 3). Five high-Ti lunar basalts have been analyzed as well (Table 2), and they have the same Fe isotope composition as terrestrial igneous rocks. The similarity in iron isotope composition of these igneous rocks indicates that igneous processes do not significantly fractionate the isotope composition of Fe, unlike the light stable isotopes, such as oxygen. Moreover, we can infer that the Fe isotope composition of the terrestrial and lunar mantles are the same, as is the terrestrial lower crust.

We use the average of the analyses for igneous rocks to define a bulk Earth-Moon Fe isotope composition of $^{54}Fe/^{56}Fe$ 0.063683 ± 17, $^{57}Fe/^{56}Fe$ = 0.023087 ± 3; and $^{58}Fe/^{56}Fe$ = 0.0030614 ± 8, which is the same as that of the J-M Fe standard, within error. Using this bulk Earth-Moon (E-M) composition as a reference, we define:

$$\delta^{56}Fe = ([^{56}Fe/^{54}Fe]_{sample}/[^{56}Fe/^{54}Fe]_{E\text{-}M} - 1)10^3.$$

We use the inverse of the measured $^{54}Fe/^{56}Fe$ ratio to follow the convention of stable isotope measurements, which define δ values for isotope ratio variations as "heavy over light" masses (e.g., δD: D/H; $\delta^{13}C$: $^{13}C/^{12}C$; $\delta^{15}N$: $^{15}N/^{14}N$; $\delta^{18}O$: $^{18}O/^{16}O$; $\delta^{34}S$: $^{34}S/^{32}S$). Use of a different set of isotope ratios such as the $^{57}Fe/^{54}Fe$ or $^{58}Fe/^{54}Fe$ are equally valid, and although use of these ratios would produce larger variations in δ values because the mass difference is larger, the errors associated with these corrected values are proportionally larger using the double-spike approach. This is also true for the empirical approach (Dixon et al., 1993).

The range of reported Fe isotope abundances for normal Fe, reported by previous workers, is highly variable. This range largely reflects the choice of instrumental mass fractionation correction (Figure 4). However, nearly all of these reported ratios can be related to one another by an exponential mass fractionation law (Figure 4), indicating that all of the Fe isotope data are within reported errors of the $^{57}Fe/^{56}Fe$ and $^{58}Fe/^{56}Fe$ measurements of this study if the variable instrumental biases are accounted for (Figure 4). The Fe isotope ratios that we use to define the bulk Earth-Moon iron reservoir are relative to the UW mixed ^{54}Fe–^{58}Fe spike, and are the most precise isotopic measurements for all four iron isotopes that have been reported (Table 2). Our reported Fe isotope ratios are the same as those reported by Taylor et al. (1992) and Walczyk (1997); the $^{54}Fe/^{56}Fe$ ratio determined in this study is within 0.2 and 1‰, respectively, of the $^{54}Fe/^{56}Fe$ ratio reported by these workers. In contrast, the $^{54}Fe/^{56}Fe$ measurements reported by Dixon et al. (1993) differ by 5‰, despite the fact that they calibrated their mass spectrometry measurements using the same method and materials as Taylor et al. (1992). The cause of the significant differences between our Fe isotope ratio measurements and those of Dixon et al. (1993) are unexplained but may in part reflect the fact that Dixon et al. (1993) measured small ion beams using an electron multiplier, in comparison to the large ion beams measured on Faraday collectors by Taylor et al. (1992); Walczyk (1997), and in this study.

In contrast to the constant Fe isotope composition of igneous rocks, the isotopic composition of Fe that has been deposited in sedimentary environments is variable, and $\delta^{56}Fe$ values range from +0.9 to −1.2 (Table 3; Figure 3). Three Fe-Mn nodules from the ocean basins have been analyzed and these samples all have $\delta^{56}Fe$ values that are significantly less than bulk planetary iron (−0.96 to −1.24). Two fresh-water nodules from Green Bay of Lake Michigan have variable $\delta^{56}Fe$ values. One Fe-rich nodule has a $\delta^{56}Fe$ value of +0.17, which is within error of the isotopic composition of E-M (igneous) Fe. The other freshwater nodule, which is Mn-rich, has a low $\delta^{56}Fe$ value of −0.59. A banded-iron formation sample from the Marquette Iron

Table 3. Corrected iron isotope compositions of Fe precipitated in sedimentary environments.*

Sample	$^{54}Fe/^{56}Fe$	% error	$^{57}Fe/^{56}Fe$	% error	$^{58}Fe/^{56}Fe$	% error	$\delta^{56}Fe$	Error (‰)
Freshwater Fe-Mn Nodules, Green Bay Lake, Michigan								
UM-GB-70-9 red Fe-nodule	0.063672	0.0117	0.023089	0.0057	0.0030619	0.0113	0.17	0.12
UM-M70-62 Black Mn-nodule	0.063721	0.0205	0.023081	0.0100	0.0030596	0.0198	−0.59	0.21
Fe-Mn Nodules from ocean basins								
Pacific Ocean Sample 1	0.063761	0.0173	0.023074	0.0084	0.0030578	0.0167	−1.22	0.17
	0.063734	0.0200	0.023078	0.0097	0.0030590	0.0193	−0.81	0.20
Pacific Ocean Sample 2	0.063769	0.0233	0.023072	0.0114	0.0030574	0.0225	−1.36	0.23
	0.063751	0.0132	0.023075	0.0064	0.0030582	0.0127	−1.06	0.13
	0.063766	0.0208	0.023073	0.0101	0.0030575	0.0201	−1.31	0.21
Atlantic Ocean Sample 3	0.063742	0.0121	0.023077	0.0059	0.0030587	0.0117	−0.92	0.12
	0.063747	0.0230	0.023076	0.0112	0.0030584	0.0222	−1.00	0.22
Banded iron formation, Maquette Range, Michigan								
Dark Layer	0.063705	0.0311	0.023083	0.0151	0.0030604	0.0300	−0.34	0.31
Light Layer	0.063631	0.0236	0.023096	0.0115	0.0030638	0.0227	0.81	0.24
	0.063642	0.0278	0.023095	0.0135	0.0030633	0.0268	0.65	0.28
	0.063632	0.0253	0.023096	0.0123	0.0030638	0.0244	0.81	0.25
	0.063597	0.0156	0.023103	0.0077	0.0030654	0.0153	1.36	0.16

* The quoted errors are internal-run statistics calculated from individual block analyses of the mixture aliquot. Replicate analyses are from different mass spectrometry runs of separate filament loads. Ocean Basin Fe-Mn nodules: sample 1 collected from a depth of 4400 meters at 16°N, 125°W; sample 2 collected from a depth of 4700 meters at 57°S, 95°W; sample 3 collected from a depth of 800 meters along the Blake Plateau.

Range, Michigan, has variable Fe isotope compositions. Light-colored and dark-colored layers that were in contact with one another were analyzed, and are different by 1.25‰; the light-colored, Fe-poor layer has a $\delta^{56}Fe$ of +0.91, whereas the dark-colored, Fe-rich layer has a $\delta^{56}Fe$ value of −0.34.

We consider biological processes to be the most likely cause of these naturally-occurring, mass-dependent iron isotope variations that are preserved in Fe that was precipitated in sedimentary environments. Ongoing experiments using iron-reducing bacteria grown on ferrihydrite substrate indicate that the ferrous iron produced by iron-reducing bacteria has a low $\delta^{56}Fe$ value (Beard et al., 1998b). It seems likely; therefore, that the Fe isotope compositions of at least some types of Fe sediments will record the isotopic composition of Fe in solution, raising the possibility that such an approach can be used to study the Fe isotope compositions of the ancient oceans, groundwater, and hydrothermal systems where biologically-induced fractionations have occurred.

6. CONCLUSIONS AND FUTURE DIRECTIONS

A precise double-spike method for determining the isotopic composition of Fe provides a rigorous correction for instrumentally-produced mass fractionation, and yet retains naturally-occurring, mass-dependent isotopic fractionation. Use of this technique allows measurement of iron isotope ratios to a precision of ±0.14‰/mass using TIMS. Fifteen terrestrial igneous rocks and five high-Ti lunar basalts have been analyzed for their iron isotope composition; these igneous rocks have the same iron isotope composition, allowing us to define a bulk Earth-Moon reservoir. In contrast, Fe that was deposited in sedimentary environments has a significant range of iron isotope compositions, which reflects naturally-produced, mass-dependent iron isotope fractionation. This is the first documented occurrence of mass-dependent isotope fractionation of Fe in nature, using high-precision, internally-consistent isotope data that have been rigorously corrected for instrumentally-produced mass fractionation. We interpret these iron isotope fractionations to be a result of biological processes, and are in the processes of conducting experiments using iron-reducing and iron-oxidizing bacteria to produce iron biominerals, which will define the extent of biological fractionation of iron isotopes.

Based on the homogeneity of the Fe isotope data for igneous rocks, it seems unlikely that equilibrium processes can produce measurable iron isotope fractionation. Therefore, the isotopic composition of iron may be an ideal geochemical fingerprint for identifying biological activity in modern or ancient environments. This observation places Fe isotope investigations at a significant advantage for tracing modern or ancient biological activity, as compared to more commonly used stable isotopes such as C, O, N, and S, which must first quantify the extent of equilibrium fractionations that are caused by temperature or other factors prior to assessing the effects of biological processes.

Acknowledgments—This research was supported by NSF grant OPP-9713968 and NASA grant NAG5-6342. We thank Carl Bowser for providing the Fe-Mn nodule samples and Phil Brown for providing the banded iron formation sample. We thank Dimitri Papanastassiou, Richard Carlson and Ariel Anbar for comments on the submitted manuscript.

REFERENCES

Beard B. L., Taylor L. A., Scherer E. E., Johnson C. M., Snyder G. A. (1998a) The source region and melting mineralogy of high-titanium and low-titanium lunar basalts deduced from Lu-Hf isotope data. *Geochim. Cosmochim. Acta* **62,** 525–544.

Beard B. L., Johnson C. M., Nealson K. H. (1998b) High precision iron isotope measurements reveals naturally occurring mass-dependent iron isotope fractionations. *Geol. Soc. Am. Abst. Prog.* **30,** A157.

Clayton R. N. (1993) Oxygen isotopes in meteorites. *Ann. Rev. Earth Planet. Sci.* **21,** 115–149.

Compston W. and Oversby V. M. (1969) Lead isotopic analysis using a double spike. *J. Geophys. Res.* **74,** 4338–4348.

Dixon P. R., Janecky D. R., Perrin R. E., Rokop D. J., Unkefer P. L.,

Spall W. D. and Maeck R. (1992) Unconventional stable isotopes: Iron. In *Water Rock Interaction volume 2: Moderate and High Temperature Environments*, pp. 915–918 (eds. Y. K. Kharaka and A. S. Maest) A. A. Balkema Publishers, Rotterdam, Netherlands.

Dixon P. R., Perrin R. E., Rokop D. J., Maeck R., Janecky D. R. and Banar J. P. (1993) Measurements of iron isotopes (^{54}Fe, ^{56}Fe, ^{57}Fe, and ^{58}Fe) in sub microgram quantities of iron. *Anal. Chem.* **65,** 2125–2130.

Eugster O., Tera F. and Wasserburg G. J. (1969) Isotopic analyses of barium in meteorites and in terrestrial samples. *J. Geophys. Res.* **74,** 3897–3908.

Friedman I. and O'Neil J. R. (1977) *Compilation of stable isotope fractionation factors of geochemical interest.* In Data Geochem, 6th edition, U.S. Geol. Survey Prof. Paper 440KK.

Gale N. H. (1970) A solution in closed form for lead isotopic analysis using a double spike. *Chem. Geol.* **6,** 305–310.

Götz A. and Heumann K. G. (1988) Iron isotope ratio measurements with the thermal ionization technique using a compact quadropole mass spectrometer. *Int. J. Mass Spectrom. Ion Processes* **83,** 319–330.

Hart S. R. and Zindler A. (1989) Isotope fractionation laws: a test using Calcium. *Int. J. Mass Spectrom. Ion Processes* **89,** 287–301.

Hoefs J. (1987) *Stable Isotope Geochemistry.* Springer Verlag, New York, 241 pp.

Hutcheon I. D., Armstrong J. T. and Wasserburg G. J. (1987) Isotopic studies of Mg, Fe, Ru, and W in Fremdlinge from Allende refractory inclusions. *Geochim. Cosmochim. Acta* **51,** 3175–3192.

Lowenstam H. A. (1981) Minerals formed by organisms. *Science* **211,** 1126–1131.

Martin J. H. and Fitzwater S. E. (1988) Iron deficiency limits phytoplankton growth in the north-east Pacific subarctic. *Nature* **353,** 331, 341–343.

McKay D. S., Gibson E. K. Jr., Thomas-Keprta K. L., Vali H., Romanek C. S., Clemett S. J., Chiller X. D. F., Maechling C. R. and Zare R. N. (1996) Search for past life on Mars: Possible relic biogenic activity in martian meteorite ALH84001. *Science* **273,** 924–930.

Miller Y. M., Ustinov V. I. and Artemov Y. M. (1966) Mass spectrometric determination of calcium isotope variations. *Geochem. Inter.* **3,** 929–933.

Russell W. A., Papanastassiou D. A. and Tombrello T. A. (1978) Ca isotope fractionation on the Earth and other solar system materials. *Geochim. Cosmochim. Acta* **42,** 1075–1090.

Schidlowski M., Hayes J. M. and Kaplan I. R. (1983) Isotopic inferences of ancient biochemistries: carbon, sulfur, hydrogen, and nitrogen. In *Earth's Earliest Biosphere: Its Origins and Evolution.* (ed. J. W. Schopf) pp 149–186. Princeton University Press, Princeton New Jersey.

Skulan J., DePaolo D. J. and Owens T. L. (1997) Biological control of calcium isotopic abundances in the global calcium cycle. *Geochim. Cosmochim. Acta* **61,** 2505–2510.

Strelow F. W. E. (1980) Improved separation of iron from copper and other elements by anion-exchange chromatography on a 4% cross-linkage resin with high concentrations of hydrochloric acid. *Tatlanta,* **27,** 727–732.

Taylor P. D. P., Maeck R., and De Bièvre P. (1992) Determination of the absolute isotopic composition and Atomic Weight of a reference sample of natural iron. *Int. J. Mass Spectrom. Ion Processes* **121,** 111–125.

Taylor P. D. P., Maeck R., Hendrickx F. and De Bièvre P. (1993) The gravimetric preparation of synthetic mixtures of iron isotopes. *Int. J. Mass Spectrom. Ion Processes* **128,** 91–97.

Valley G. E. and Anderson H. H. (1947) A comparison of the abundance ratios of the isotopes of terrestrial and meteoritic iron. *J. Am. Chem. Soc.* **69,** 1871–1875.

Völkening J. and Papanastassiou D. A. (1989) Iron isotope anomalies. *Astrophys. J.* **347,** L43–L46.

Walczyk T. (1997) Iron isotope ratio measurements by negative thermal ionization mass spectrometry using FeF_4^- molecular ions. *Int. J. Mass Spectrom. Ion Proc.* **161,** 217–227.